ISSN : 1226-7244 (Print)
ISSN : 2288-243X (Online)
논문번호 18-03-36
238
j.inst.Korean.electr.electron.eng.Vol.22,No.3,759~766,September 2018
http://dx.doi.org/10.7471/ikeee.2018.22.3.759

Design and Analysis of a Material Efficient Sinusoidal Consequent-Pole High-Speed Axial-Flux Machine

Sunil Kumar*, Byung-il Kwon*★

Abstract

This paper presents a high-speed axial-flux machine which utilizes the idea of sinusoidal shaped pole combined with a consequent iron-pole. The target of the proposed machine is the cost reduction of the relatively expensive Samarium-Cobalt (SmCo) permanent magnet (PM) material and the torque per PM volume improvement by using sinusoidal consequent-pole rotor. The effectiveness of the proposed machine is validated by comparing it with conventional consequent-pole and with conventional PM machines using 3-D finite element method (FEM) simulations. The comparison and analysis is done in terms of back electro-motive force (back-EMF) harmonic contents, torque per PM volume and torque ripple characteristics. The simulation results show that the proposed machine is suitable and cost-effective for high-speed and high torque per PM volume applications. Furthermore, due to the consequent pole, the magnetic flux saturation and the overload current torque-capability are also presented and discussed in the paper.

Key words : High-speed axial-flux machine, Flywheel energy storage system, Consequent-pole machine, Sinusoidal back-EMF, Torque-per-PM volume, and 3-D finite element method

Ⅰ. Introduction

Rare-earth permanent magnet (PM) machines provides a robust rotor structure, high torque density and removal of slip rings and brushes from the conventional wound rotor synchronous machines. With the advancement in the high grade rare-earth PMs (NdFeB and SmCo), the PM machines became capable of providing high torque density and simpler rotor structure in electrical machines [1]-[3]. However, the rare-earth PM machines suffered the drawback of high cost and fluctuating supply of the PMs. High speed PM machines have been considerably researched for flywheel energy storage systems (FESS) in which the energy is stored in the form of kinetic energy in a rotating flywheel [4]-[9]. FESS have been researched in the areas specializing in electrical power systems, automobiles, satellite systems, etc. [8], [9]. In satellite systems, flywheels are a promising technology when compared with the chemical batteries in terms of charge and discharge cycles, life-time expectancy and non-toxic chemical composition.

* Department of Electronic Systems Engineering, Hanyang University.
★ Corresponding author
E-mail : bikwon@hanyang.ac.kr, Tel : +82-31-400-5165
※ Acknowledgment
This work was supported in part by the Human Resources Program in Energy Technology of the Korea Institute of Energy Technology Evaluation and Planning (KETEP), granted financial resource from the Ministry of Trade, Industry & Energy, Republic of Korea. (No.20154030200730), and in part by the BK21PLUS Program through the National Research Foundation of Korea within the Ministry of Education.
Manuscript received Sep. 07, 2018; revised Sep. 19, 2018; Accepted Sep. 20, 2018

High speed machines give rise to high operating temperatures. The SmCo PMs becomes a best choice to withstand the high temperature conditions as well as the high magnet remanent flux density. Therefore, it is always a desirable to use the SmCo PMs for high speed and high torque density applications such as FESS. Due to high cost and uncertain availability of rare-earth PMs, the researchers are focusing on the employment of non-PM or reduced-PM machines [10], [11]. Consequent pole machines have been recently researched due to their better torque performances while reducing the number of PMs in various electric machines [10]-[15]. However, the consequent pole machines have not yet been researched for high speed applications.

Axial flux permanent magnet (AFPM) machine has been evolved as an efficient design considering the higher torque density, simple pan-cake structure, and better self-cooling mechanism. The stator and the rotor can be arranged in various configurations such as single-rotor and single-stator, dual-rotor and single stator, dual-stator and single-rotor, etc. AFPM machines have been specifically researched for flywheel application due to their unique features. Its axial force can be primarily adjusted and controlled to counter against the weight of the rotor if the rotor is vertically oriented. The PMs in the two rotors are kept at slightly unequal thickness to generate a net axial force which balances the weight of the rotor. This reduces the bearing stress and thereby minimize the mechanical frictional losses at high speed operation. This is crucial for the loss reduction in flywheel since the flywheel normally operates in steady state mode at high speed [16]-[18].

A dual-rotor and single-stator AFPM machine model with sinusoidal shaped PM poles has been presented in [19], [20]. The sinusoidal shaped PMs induces sinusoidal back EMF in the stator windings and hence, minimizing the torque ripples of the machine.

In this paper, a high speed axial-flux machine for FESS is proposed which utilize the idea of consequent-pole along with the sinusoidal pole shape to reduce the cost of the relatively expensive SmCo PMs. The consequent pole machine improves the torque per PM volume, whereas the sinusoidal shaped pole retains the sinusoidal back-EMF waveform shape and the low torque ripples. Hence, the proposed machine will improve the torque per PM volume density without deteriorating the back-EMF shape and the torque ripples.

II. Proposed Sinusoidal Consequent-Pole Axial-Flux Machine

The proposed two-stator and two-rotor axial-flux machine is shown in Fig. 1. This axial-flux machine has two-pole rotors with sinusoidal shaped poles. The sinusoidal shaped poles induce sinusoidal back electro-motive force (back-EMF) in the stator windings [19]. The two-pole machine exhibits the lowest possible operating frequency so that the electrical losses should be kept minimum. Furthermore, the cogging torque is absent due to the slotless stator design. Hence, the machine possesses almost zero torque ripple feature due to the sinusoidal back-EMF and the absence of cogging torque. Therefore, the machine inheres the ideal design for high speed applications such as FESS.

The stator is designed to have simple slotless structure with toroidal three-phase winding as shown in Fig. 1(a). Both the stators, lower stator and upper stator, are of same dimensions and winding configuration.

The stator windings from the two stators are supplied from a single inverter and are connected in series with the corresponding phases as shown in the circuit diagram of Fig. 1(b). The stator is supplied with a rated sinusoidal current of 10 A-peak with 533.33 Hz rated frequency for 32,000 rpm rotor speed. The two rotors are

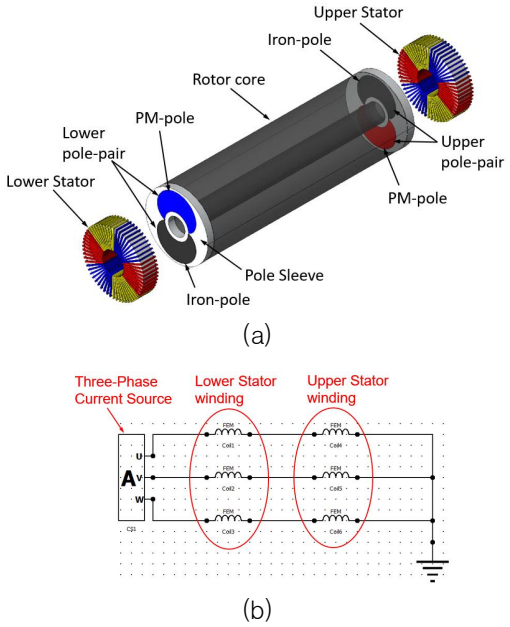

Fig. 1. The proposed high speed axial flux machine. (a) Topology (b) Circuit diagram

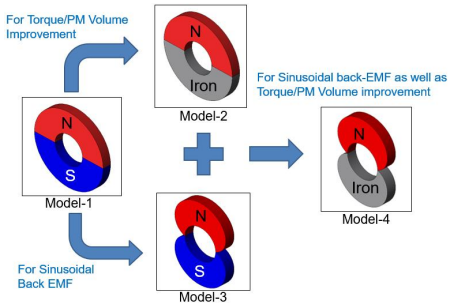

Fig. 2. Investigated rotor pole shapes and their design process.

designed to form an integrated mechanical structure comprising of upper and lower pole pairs, aluminum sleeve, and rotor core. The upper and lower pole pairs are designed to have unequal thicknesses so that the rotor can generate a net axial force in vertical direction. The net axial force is generated to primarily counteract against the weight of the vertically oriented rotor. This idea is used to minimize the bearing stress [16]-[18]. A sleeve is designed, made up of aluminum metal, to hold the rotor pole pairs in their position at high speed operation. Aluminum is used as a sleeve material due to its permeability equal to the air and to reduce the mechanical stress of the rotor. The

Table 1. Machine Dimensions and Specifications

Item	Unit	Model1	Model2	Model3	Model4
Stator Outer Diameter	mm	70			
Stator Inner Diameter	mm	28			
Rotor Outer Diameter	mm	74			
Shaft Diameter	mm	20			
Upper poles thickness	mm	8.0			
Lower poles thickness	mm	7.6			
Airgap length	mm	0.5			
Rotor Speed for Analysis	RPM	32,000			
PM Remanent Flux Density	T	1.02			
Total PM volume	mm3	50430	25215	32106	16053

mechanical effectiveness of the sleeve is verified using FEM mechanical stress analysis [20]. The rotor core is designed to serve two purposes. Firstly, it serves as back-iron for both the upper and lower pole pairs without interacting with each other. Secondly, it can be used as a flywheel mass in this fashion using the same material to have mechanical integrity for the high speed rotor.

In order to evaluate the performance of the proposed machine, four machine models are presented. These machine models are based on different rotor pole shapes and their material as shown in Fig. 2. The stator dimensions, winding configuration, and all other dimensions are kept the same in all models. Model-1 is based on the conventional ring shaped PM pole pair rotor with SmCo PMs. Model-2 is based on the ring shaped PM and the consequent iron-pole pair rotor. Model-3 is based on the sinusoidal shaped PM pole pair rotor with SmCo PMs. The proposed Model-4 is based on the sinusoidal shaped PM and the consequent iron-pole pair concept.

III. 3-D FEM Simulation Results and Comparison

3.1 Flux Density

The magnetic flux density plots in the rotor pole pair of all four models are shown in Fig. 3. The PM material used in all the models is SmCo (Br=1.02T). The flux density in the ring shaped PM pole of Model-1 is uniformly distributed due to the inherent property of the PM. Whereas, the flux density in the consequent iron-pole of Model-2 is slightly disturbed due the PM and the consequent iron-pole pair combination. The maximum flux density is found to be at the boundary between the PM and the consequent iron-pole of Model-2 rotor. The maximum flux density value in Model-2 is found to be 1.9 T which is under the saturation limits of the consequent iron-pole. Besides the boundary, the flux density in major part of the consequent iron-pole is uniformly distributed. Similarly, the flux density in the sinusoidal PM pole of Model-3 is uniformly distributed. Whereas, in case of Model-4 in which consequent iron-pole is used, the flux density is concentrated near the boundary of the PM and the consequent iron-pole. However, in this case, the boundary of the PM and the consequent iron-pole is quite small as compared to that of the Model-2.

3.2 Axial Force

The presented four models utilize the upper and lower rotor poles with unequal thicknesses as mentioned in Table-1. The unequal PM thickness generates a net axial force along the axis of rotation. The net axial force is generated so that it can primarily balance the weight of the rotor when the rotor is vertically oriented. The net axial forces are simulated and presented in Fig. 4 for all the four models. The net axial force generated by Model-1 rotor is calculated as 9.4 N whereas that of Model-2 rotor as 13.8 N. The increase in the net force is due to the change in

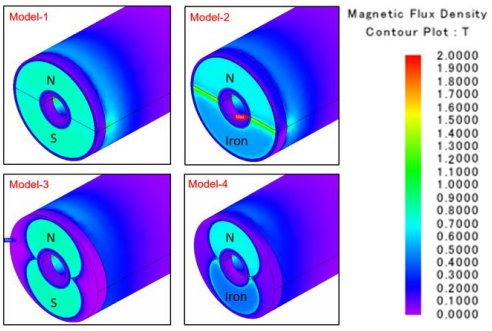

Fig. 3. Magnetic flux density plots of the investigated models.

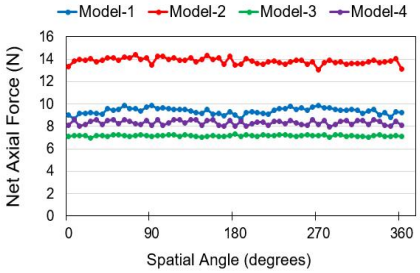

Fig. 4. Net axial force of the investigated models.

permeance of the magnetic circuit due to the introduction of the consequent iron-pole in Model-2. Similarly, the net axial force is increased in sinusoidal shaped poles of Model-4 as compared to Model-3 as shown in Fig. 4. However, the net axial force can be adjusted by varying the thicknesses of either of the upper or the lower poles as required. The net axial force of Model-4 is found to be 8.33 N which approximately equal to the weight of the rotor which is 8.37 N. This will minimize the bearing loss due to the weight of the high-speed rotor.

3.3 Radial Force

There exists a certain amount of radial forces in case of Model-2 and Model-4 due to the consequent iron-pole rotor. The radial force is generated due to the different value of magnetic flux in the PM and the consequent pole pair combination. However, the due to the opposite placement of the PM and the consequent poles in the upper and lower pole pairs, the net radial force becomes zero. The radial forces for the Model-2

and Model-4 are simulated over one rotation and shown in Figs. 5(a) and 5(b), respectively.

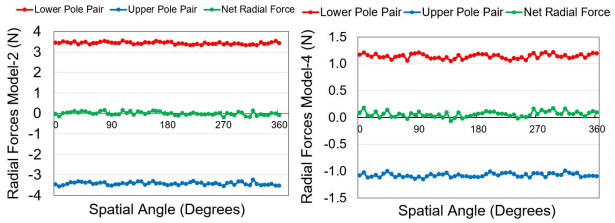

(a) (b)

Fig. 5. Radial forces due to the consequent iron-pole rotor. (a) Model-2 (b) Model-4.

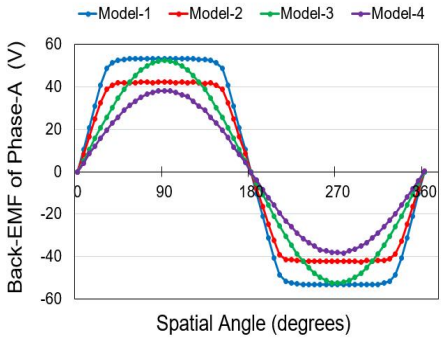

Fig. 6. Back-EMFs of Phase-A of the investigated models.

3.4 Back-EMF

The open circuit back-EMF is simulated at the rated speed for all the four models and is shown in Fig. 6. The back-EMF waveform shape of the basic models i.e., Model-1 and Model-2 is of square shape due to the ring shaped rotor poles. The back-EMF waveform shape of Model-3 and Model-4 is of sinusoidal shape due to the sinusoidal shaped rotor poles. As can be noticed from the Fig. 6, the back-EMF waveform shape does not change by using the consequent iron-poles. Also, the total harmonic distortion (THD) factor remains the same in case of Model-1 and Model-2 due to the ring shaped poles. Similarly, in case of Model-3 and Model-4, the back-EMF THD factor remains the same due to sinusoidal shaped poles. The back-EMF root mean square (RMS) and the THD factor values of all the models are presented in Table-2.

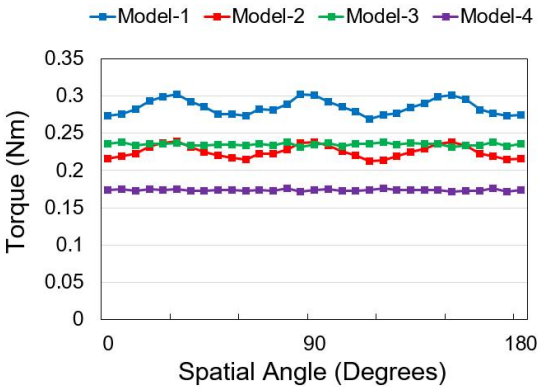

Fig. 7. Electromagnetic torque curves of the investigated models.

3.5 Electromagnetic Torque

The electromagnetic torque is computed by applying the rated current to the stator windings. The electromagnetic torque waveforms of all the four models are shown in Fig. 7. The torque ripples are due to the harmonics present in the corresponding back EMF waveform. The average torque values and the torque ripple factor (TRF) is calculated and summarized in Table-2. The TRF of the Model-1 and Model-2 is found to be the same due to the same back-EMF THD factor of the respective models. This shows that by using consequent iron-pole rotor, the machine TRF does not change. The average torque is reduced in Model-2 as compared to Model-1, however the torque per PM volume density is increased due to the consequent iron-pole as shown in Table-2. Similarly, the TRF of the Model-4 does not change from the Model-3, however the torque per PM volume density is increased not only from the Model-3 but from the Model-2 as well. This shows that by using the sinusoidal shaped pole as well as the consequent iron-pole concept the torque per PM volume density gives the highest value. The torque per PM volume comparison of all four models is shown in Fig. 8 which shows that Model-4 provides the highest value of torque per PM volume. This proves the effectiveness of the proposed machine by reducing the magnet size and improving the torque per PM volume density.

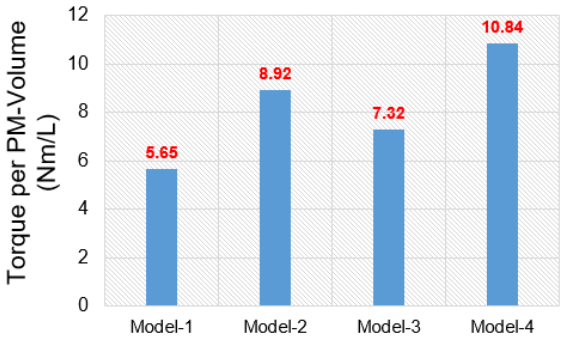

Fig. 8. Torque per PM volume comparison.

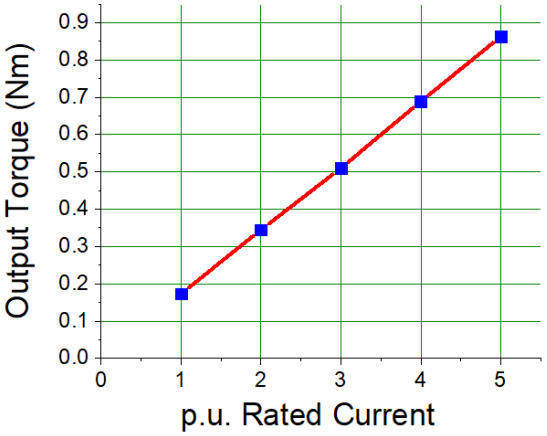

Fig. 9. Overload current torque capability performance.

Table 2. 3-D FEM Performance Comparison.

Item	Unit	Model 1	Model 2	Model 3	Model 4
Back EMF RMS Value	V	46.3	36.8	36.9	27.26
Back EMF THD	%	20.9	21.3	0.68	0.97
Torque Ripple Factor	%	11.21	10.66	2.64	2.30
Average Torque	Nm	0.285	0.225	0.235	0.174
Total PM volume	mm3	50430	25215	32106	16053
Torque per PM Volume	Nm/L	5.65	8.92	7.32	10.84

3.6 Overload Capability

The proposed Model-4 employs the consequent iron-poles. Due to rapid charging and discharging of the FESS, the current in the machine can be overloaded. The overload current can cause the magnetic flux in the consequent iron-pole to reach the saturation limit, thereby decreasing the torque output. Therefore, it is important to ensure the overload current performance of the machine. In this condition, the proposed Model-4 is analyzed with an overload current of up to 5 times the rated current and the corresponding torque output is calculated. Fig. 9 shows the output torque versus the per-unit (p.u.) rated current. The output torque varies linearly with the increase in the applied overload current. The response curve shows that the proposed machine can withstand the overload current without the saturation of the iron poles.

IV. Conclusion

In this paper, an axial-flux sinusoidal consequent pole machine is proposed for high speed flywheel application. The proposed machine utilizes the idea of both the sinusoidal shaped pole as well as the consequent iron pole. The consequent pole is used to reduce the cost of the expensive SmCo PMs and improve the torque per PM volume. The proposed machine is then compared with conventional PM and consequent pole machines in terms of back-EMF harmonics and torque characteristics. The 3D-FEM results show that the proposed machine can provide higher torque per PM volume than that of both the conventional PM and the consequent pole machines without affecting the back EMF harmonics and the torque ripples. Furthermore, the proposed machine can withstand the overload current torque capability without being saturated due to the iron-poles. Hence, the proposed sinusoidal consequent pole machine is suitable and cost effective for high speed and high torque per PM volume density applications.

References

[1] L. Gu, W. Wang, B. Fahimi and M. Kiani, "A Novel High Energy Density Double Salient

Exterior Rotor Permanent Magnet Machine," *in IEEE Transactions on Magnetics,* vol.51, no.3, pp.1-4, 2015. DOI:10.1109/TMAG.2014.2366081
[2] C. Hwang, S. Hung, C. Liu and S. Cheng, "Optimal Design of a High Speed SPM Motor for Machine Tool Applications," *in IEEE Transactions on Magnetics*, vol.50, no.1, pp.1-4, 2014. DOI:10.1109/TMAG.2013.2276092
[3] J. Rao, L. Zhang and G. Zhou, "Rotor design and optimizations for interior permanent magnet machines in motorized spindle application," *20th International Conference on Electrical Machines and Systems (ICEMS)*, Sydney, NSW, pp.1-5, 2017. DOI:10.1109/ICEMS.2017.8056347
[4] W. Wang, H. Hofmann, and C. E. Bakis, "Ultrahigh Speed Permanent Magnet Motor/ Generator for Aerospace Flywheel Energy Storage Applications," *IEEE Int. Conf. Electr. Mach. Drives*, pp.1494-1500, 2005. DOI:10.1109/IEMDC.2005.195918
[5] C. Zwyssig, J. W. Kolar, and S. D. Round, "Megaspeed Drive Systems: Pushing Beyond 1 Million r/min," *IEEE/ASME Trans. Mechatronics*, vol.14, no.5, pp.564,574, 2009. DOI:10.1109/TMECH.2008.2009310
[6] A. Tuysuz, C. Zwyssig, and J. W. Kolar, "A Novel Motor Topology for High-Speed Micro-Machining Applications," *IEEE Transactions on Industrial Electronics*, vol.61, no.6, pp.2960-2968, 2014. DOI:10.1109/TIE.2013.2273481
[7] D. Krähenbühl, C. Zwyssig, H. Weser, and J. W. Kolar, "A Miniature 500 000-r/min Electrically Driven Turbocompressor," *IEEE Transactions on Industry Applications*, vol.46, no.6, pp.2459-2466, 2010. DOI:10.1109/TIA.2010.2073673
[8] M. A. Awadallah and B. Venkatesh, "Energy Storage in Flywheels: An Overview," *Canadian Journal of Electrical and Computer Engineering*, vol.38, no.2, pp.183-193, 2015. DOI:10.1109/CJECE.2015.2420995
[9] R. Hebner, J. Beno and A. Walls, "Flywheel batteries come around again," *IEEE Spectrum*, vol.39, no.4, pp.46-51, 2002. DOI:10.1109/6.993788
[10] A. Hussain, S. Atiq and B. I. Kwon, "Consequent-Pole Hybrid Brushless Wound-Rotor Synchronous Machine," in *IEEE Transactions on Magnetics,* 2018. DOI:10.1109/TMAG.2018.2837690
[11] I. Boldea, L. N. Tutelea, L. Parsa, and D. Dorrell, "Automotive electric propulsion systems with reduced or no permanent magnets: An overview," *IEEE Transactions on Industrial Electronics*, vol.61, no.10, pp.5696 - 5711, 2014. DOI:10.1109/TIE.2014.2301754
[12] Y. Gao, R. Qu, D. Li, J. Li and G. Zhou, "Consequent-Pole Flux-Reversal Permanent Magnet Machine for Electric Vehicle Propulsion," in *IEEE Transactions on Applied Superconductivity*, vol.26, no.4, pp.1-5, 2016. DOI:10.1109/TASC.2016.2514345
[13] Yolacan and M. Aydin, "Rotor Design Optimization of a New Flux-Assisted Consequent Pole Spoke-Type Permanent Magnet Torque Motor for Low-Speed Applications," in *IEEE Transactions on Magnetics,* 2018. DOI:10.1109/TMAG.2018.2832076
[14] N. Baloch, B. I. Kwon and Y. Gao, "Low-Cost High-Torque-Density Dual-Stator Consequent-Pole Permanent Magnet Vernier Machine," in *IEEE Transactions on Magnetics,* 2018. DOI:10.1109/TMAG.2018.2849082
[15] C. Shi, D. Li, R. Qu, H. Zhang, Y. Gao and Y. Huo, "A Novel Linear Permanent Magnet Vernier Machine With Consequent-Pole Permanent Magnets and Halbach Permanent Magnet Arrays," in *IEEE Transactions on Magnetics*, vol.53, no.11, pp.1-4, 2017. DOI:10.1109/TMAG.2017.2696559
[16] T. D. Nguyen, K. J. Tseng, S. Zhang and H. T. Nguyen, "A Novel Axial Flux Permanent-Magnet Machine for Flywheel Energy Storage System: Design and Analysis," *IEEE Transactions on Industrial Electronics*, vol.58, no.9, pp.3784-3794, 2011. DOI:10.1109/TIE.2010.2089939
[17] T. D. Nguyen, G. Foo, K. J. Tseng and D. M. Vilathgamuwa, "Modeling and Sensorless Direct Torque and Flux Control of a Dual-Airgap Axial Flux Permanent Magnet Machine With Field-

Weakening Operation," *IEEE/ASME Transactions on Mechatronics*, vol.19, no.2, pp.412-422, 2014. DOI:10.1109/TMECH.2013.2242481

[18] T. D. Nguyen, K. J. Tseng, S. Zhang and H. T. Nguyen, "On the modeling and control of a novel flywheel energy storage system," *2010 IEEE International Symposium on Industrial Electronics*, pp.1395-1401, 2010. DOI:10.1109/ISIE.2010.5637797

[19] S. Kumar, W. Zhao, Z. Du, T. A. Lipo, and B. I. Kwon, "Design of Ultra-high Speed Axial Flux Permanent Magnet Machine with Sinusoidal Back-EMF for Energy Storage Application," *IEEE Transactions on Magnetics,* vol.51, no.11, pp.1-4, 2015. DOI:10.1109/TMAG.2015.2451162

[20] S. Kumar, T. A. Lipo and B. I. Kwon, "A 32,000 r/min Axial Flux Permanent Magnet Machine for Energy Storage With Mechanical Stress Analysis," *IEEE Transactions on Magnetics*, vol.52, no.7, pp.1-4, 2016. DOI:10.1109/TMAG.2015.2512939

BIOGRAPHY

Sunil Kumar (Member)

2011 : B.E. degree in Electrical Engineering, NED University, Karachi, Pakistan.
2013 : MS and PhD degree candidate in Electronic Systems Engineering, Hanyang University, Ansan, South Korea.
2012~2013 : Trainee Engineer, Karachi Electric Supply Company, Pakistan.

Byung-il Kwon (Member)

1981 : BS degree in Electrical Engineering, Hanyang University, South Korea.
1983 : MS degree in Electrical Engineering, Hanyang University, South Korea.
1989 : PhD degree in Electrical Engineering, University of Tokyo, Japan.
1991~to date : Professor, Hanyang University, Ansan, South Korea.